This is a peer reviewed version of an article published by Taylor & Francis. The published version of Jesús Balado, Celia Olabarria, Joaquín Martínez-Sánchez, José R. Rodríguez-Pérez & Arias Pedro (2021) Semantic segmentation of major macroalgae in coastal environments using high-resolution ground imagery and deep learning, International Journal of Remote Sensing, 42:5, 1785-1800 is available at https://doi.org/10.1080/01431161.2020.1842543

Semantic segmentation of major macroalgae in coastal environments using high-resolution ground imagery and deep learning

Jesús Balado[a*], Celia Olabarria[b,c], Joaquín Martínez-Sánchez[a], José R. Rodríguez-Pérez[d], Pedro Arias[a]

[a]Universidade de Vigo. CINTECX. Campus universitario de Vigo, As Lagoas, Marcosende 36310 Vigo, Spain

[b] Universidade de Vigo, Departamento de Ecoloxía e Bioloxía animal, Facultade de Ciencias do Mar. Campus Lagoas-Marcosende, s/n, 36310 Vigo, Spain

[c] Universidade de Vigo. CIM, Centro de Investigación Mariña. Illa de Toralla, s/n, 36331 Vigo, Spain
[d]Universidad de León. GEOINCA. Avenida de Astorga, s/n, 24401 Ponferrada, Spain

[*] Correspondig autor.

E-mail address: jbalado@uvigo.es (J. Balado)

Abstract

Macroalgae are a fundamental component of coastal ecosystems and play a key role in shaping community structure and functioning. Macroalgae are currently threatened by diverse stressors, particularly climate change and invasive species, but they do not all respond in the same way to the stressors. Effective methods of collecting qualitative and quantitative information are essential to enable better, more efficient management of macroalgae. Acquisition of high-resolution images, in which macroalgae can be distinguished on the basis of their texture and colour, and the automated processing of these images are thus essential. Although ground images are useful, labelling is tedious. This study focuses on the semantic segmentation of five macroalgal species in high-resolution ground images taken in 0.5 x 0.5 m quadrats placed along an intertidal rocky shore at low tide. The target species, *Bifurcaria bifurcata*, *Cystoseira tamariscifolia*, *Sargassum muticum*, *Sacchoriza polyschides* and *Codium* spp., which predominate on intertidal shores, belong to different morpho-functional groups. The study explains how to convert vector-labelled data to raster-labelled data for adaptation to convolutional neural network (CNN) input. Three CNNs (MobileNetV2, Resnet18, Xception) were compared, and ResNet18 yielded the highest accuracy (91.9%). The macroalgae were correctly segmented, and the main confusion occurred at the borders between different macroalgal species, a problem derived from labelling errors. In addition, the interior and exterior of the quadrats were correctly delimited by the CNNs. The results were obtained from only one hundred labelled images and can be performed on personal computers, without the need to resort to external servers. The proposed method helps automation of the labelling process.

Keywords: Macroalgae; intertidal rocky shore; convolutional neural networks; image processing; semantic segmentation

1. Introduction

Macroalgae are important primary producers on subtidal and intertidal rocky shores worldwide (Jenkins et al., 2008) and make a substantial contribution to carbon sequestration, nutrient cycling and global oxygen production (Bañolas et al., 2020; Macreadie et al., 2017). As ecosystem engineers, they modify habitat conditions, facilitating the existence and survival of other intertidal species and thus strongly influencing the structure and functioning of coastal ecosystems (Purvaja et al., 2018). They also provide food, shelter and nursery grounds for many invertebrate and vertebrate species, including commercially important species (Smale et al., 2013).

Macroalgae also provide various, highly valuable ecosystem services to humans (Beaumont et al., 2008; Quiros et al., 2018). They are highly nutritious and produce bioactive compounds used in fertilizers, food and medical and cosmetic products (Rebours et al., 2014). Macroalgae are also beginning to be considered as a renewable energy source and as an alternative to fossil fuels (algal biofuel) (Adeniyi et al., 2018; Debiagi et al., 2017). The main benefit of algal biofuel is that it is CO_2 neutral as the CO_2 emitted to the atmosphere during biofuel combustion is equivalent to CO_2 needed by the algae to grow and be converted into biofuel. In addition, compounds extracted from macroalgae can be used to neutralize harmful substances from water, at a much smaller cost than other methods. Some authors have reported that algal biofuel can be generated during the use of algae in wastewater treatment (Park et al., 2011; Pittman et al., 2011).

Coastal and nearshore loss of biodiversity is occurring as a consequence of diverse stressors, including climate change, habitat loss, eutrophication, overfishing, pollution and the introduction of non-native species (Griffiths et al., 2020; Hawkins et al., 2009). Intertidal species of macroalgae are vulnerable to these stressors because they are already close to their physiological tolerance thresholds during consecutive periods of emersion and immersion (Helmuth et al., 2006). Shifts in the distributional range of diverse intertidal macroalgae due to increased air and sea surface temperatures (SSTs) on the Atlantic shores of the Iberian Peninsula have been documented (Duarte et al., 2013; Lamela-Silvarrey et al., 2012; Lima et al., 2007).

Given the ecological importance of macroalgae and the large number of uses that have been identified, obtaining information about their distribution and abundance is important for monitoring, managing and understanding coastal ecosystems, particularly in the context of global change, in which multiple stressors act together (Floor et al., 2018). Video and photographic monitoring have proven valuable ground-based and remote-sensing techniques for evaluating the cover and distribution of coastal organisms with high spatial and temporal resolution, by using satellites (Li et al., 2012; Sagawa et al., 2012; Topouzelis et al., 2016; Wang et al., 2018; Wilson et al., 2019), UAVs (Duffy et al., 2018; Taddia et al., 2019; Tamondong et al., 2018; Ventura et al., 2018; Wang et al., 2019) or underwater drones (Kellaris et al., 2019; Martin-Abadal et al., 2018; Moniruzzaman et al., 2019; Rahnemoonfar and Dobbs, 2019). Satellite monitoring is useful for mapping large areas as it provides wide coverage, spatio-temporal refreshment of a few days, often at visible and infrared wavelengths, and requires less input of time and labour than traditional surveys (Schroeder et al., 2019). However, because of the patchiness of macroalgae, especially on intertidal shores (Matias et al., 2015), many species are not recognizable at the resolution of satellite images, unless they cover large areas and are different colours (Brodie et al., 2018). Thus, studies based on aerial data only can monitor biomass or blooms of one species (Xing et al., 2019). Due to the rapid progress of these technologies, the spatial resolution of colour images and the size of image archives are increasing yearly. More sophisticated and efficient image processing algorithms and methods are therefore urgently needed.

The use of photograph-based technology for monitoring coastal organisms, including macroalgae and seagrasses, is increasingly being reported. For instance, seaweeds and seagrasses have been mapped using optical processing techniques and textures (Kakuta et al., 2016). Local Binary Patterns (LBP) and Histogram of Oriented Gradients (HOG) have also been implemented as a feature extractor for segmentation of plant species in wetlands (Wang et al., 2018) or in underwater environments (Reus et al., 2018). Calculation of indices such as the Normalized Difference Vegetation Index (NDVI), the Floating Algae Index (FAI) and the Seaweed Enhancing Index (SEI) can be also used for feature extraction (Siddiqui et al., 2019).

Traditional image processing techniques for detecting and classifying macroalgae are being displaced by machine learning and deep learning methods, which provide more accurate results (O'Byrne et al., 2018; Reus et al., 2018). Deep learning based techniques are limited by the large numbers of samples needed to train the classifier. To differentiate species of macroalgae, samples must be acquired using traditional approaches based on field data, such as diving or intertidal sampling, with in situ quadrats or line transects, which provide high accuracy and resolution, but which are time consuming and limited to small areas (Casal et al., 2013).

The aim of this study was to automate the process of labelling high-resolution images to differentiate five macroalage: *Bifurcaria bifurcata* Linnaeus, *Cystoseira tamariscifolia* (Hudson) Papenfuss, *Sargassum muticum* (Yendo) Fensholt, *Sacchoriza polyschides* (Lightfoot) Batters, and *Codium* spp. The process was automated using semantic segmentation and convolutional neural networks (CNNs). To our best knowledge, no other works have previously addressed semantic segmentation of five macroalgal species at once from ground, aerial or satellite images. This paper presents a new method of converting labels (from polygons to raster images) and compares the results obtained with three different CNNs (MobileNetV2, Resnet18, Xception). This work is part of ALGANAT2000 project, which aims to monitor the spatio-temporal distribution of macroalgae in an intertidal coastal area within a marine protected area in Galicia (NW Spain) during 2019.

2. Material and Methods

2.1. Study area

The study was conducted in the Atlantic Islands National Park (Galicia, NW Spain), a terrestrial and marine reserve formed by four main archipelagos. The exposed intertidal area of Bufardo on the Illa de Monteagudo (area surrounding coordinates 42.23551° N, 8.89956 °W) belonging to the Illas Cíes archipelago was the selected as the sampling location (Figure 1). The location is a gently sloping rocky platform with the upper intertidal dominated by *Pelvetia canaliculata* Decaisne and Thuret, and the mid and low intertidal areas are dominated by conspicuous red, green and brown macroalgae, such as *Asparagopsis armata* Harvey, *B. bifurcata*, *C. tamariscifolia*, *S. polyschides* and *Codium* spp.

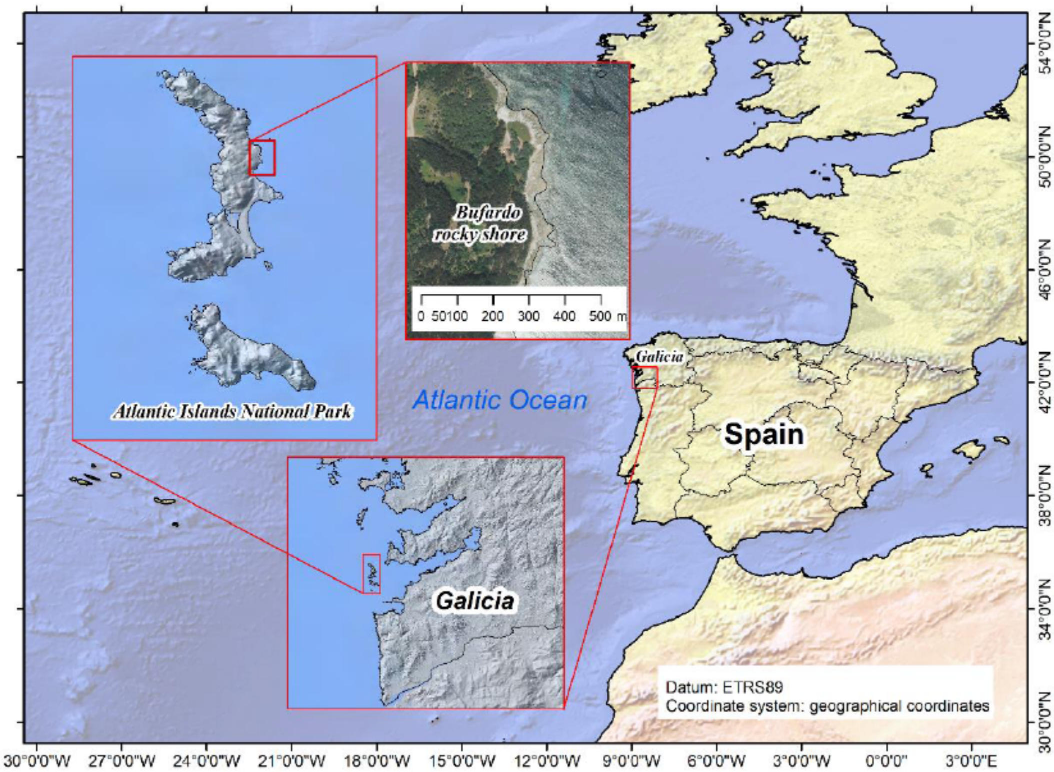

Figure 1. Location of the Bufardo rocky shore in the Atlantic Islands National Park (Galicia, Spain).

The images of the five species (Figure 2) were acquired from 0.5 x 0.5 m quadrats placed on the low intertidal shore during low spring tides in July, August and September 2019. The area is emerged, and thus exposed to the air, for about 3-3.5 hours during low spring tides. Depending on the altitude at which the macroalgae occur on the shore, they experience different conditions of solar radiation and desiccation. Thus, macroalgae living on the upper shore are drier and absorb more heat than macroalgae inhabiting the lower shore.

B. bifurcata | *C.tamariscifolia* | *S. muticum* | *S. polyschides* | *Codium* spp

Figure 2. Target macroalgae used in the semantic segmentation.

The images were acquired with a Fujifilm FinePix JV200 camera mounted on a tripod, with a top view perspective 0.7 m above the ground (see Figure 3). Because of the shape of the tripod, the base was also captured in each image. The square base delimited the labelling area, and the area outside of the base was labelled as the "out" class.

Figure 3. Quadrat used for image acquisition.

2.2. Methods

Labelled data (in the form of manually digitized georeferenced vector polygons) and high-resolution images of macroalgae were used for semantic segmentation. Vector labelled data were adapted to raster labelled data following convolutional neural network (CNN) standards. The choice of CNN was justified by the higher success rate than those of other traditional methods based on texture analysis (O'Byrne et al., 2018), histogram of oriented gradients (HOG), local binary patterns (LBP) (Reus et al., 2018). In addition, pre-trained CNNs also enable more efficient feature extraction, with a faster design process than traditional techniques (assembly of successive masks with successive tests). The analysis was approached from the perspective of data analysis, and the system improved as new CNN architectures become available without the entire work process having to be redesigned. The workflow of the method is represented in Figure 4.

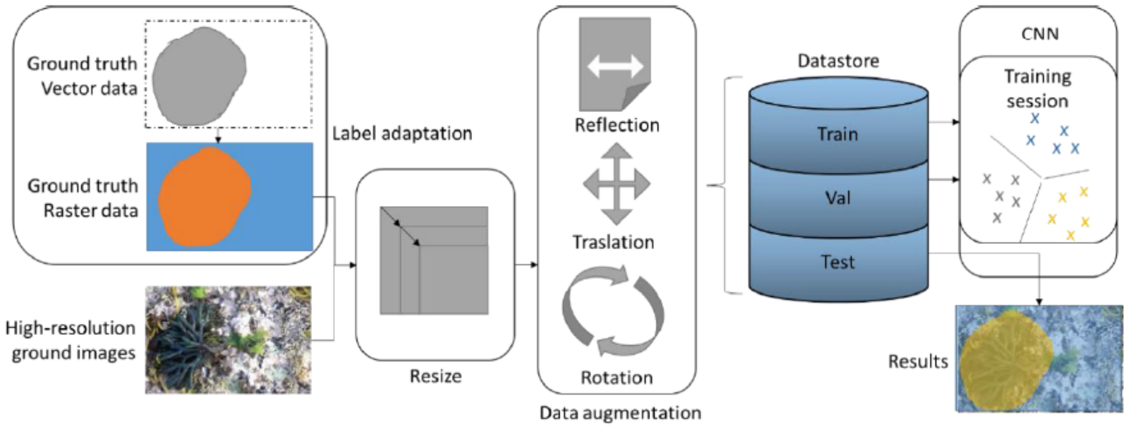

Figure 4. Workflow

2.2.1. Label adaptation for CNN

Conventional labelling of vector objects with a geographic information system (GIS) is not suitable for CNN-based semantic segmentation. The conventional method consists of creating a vector file layer with polygons labelled with the class. These polygons are delimited, by an expert, on the background image collected in the field. Apart from their topological attributes, the only condition for labelling is that the polygons must contain only one class of pixels. The expert selects which pixels to polygonise (for training the subsequent class). As a result, the expert classification is considered ground truth and consists of a labelled vector layer.

CNN for semantic segmentation only allows images (raster data) as input for both ground truth and labelled data. In addition to the data type, the labelling content is distinct and must obey the following rules:

- All pixels in the image must be labelled. Unlabelled pixels are assigned as "others". The "others" class may include macroalgae that are not of interest for the study, e.g. sand, rocks and unidentified objects.
- All pixels of the objects must be labelled in their corresponding class. The "others" class must not include pixels representing objects belonging to any class.

In order to fulfil these requirements for CNN training, each image was re-labelled accordingly. The re-labelling procedure depended on the following scenarios that can occur in each image-labelled data:

- The expert only polygonised the largest or most relevant macroalgae. In this option, the other pixels must be manually analysed and assigned to the corresponding class (whether macroalgae or *"others"*).
- The expert polygonised both large and small objects. In this case, only the data corresponding to ground and no relevant species need to be labelled *"others"*. In this option, the process could be performed automatically by rasterizing the polygons.

Considering that the option used for each image was not known, the re-labelling process was performed manually. In addition, due to the image acquisition method used, macroalgae were labelled exclusively in a region of interest (ROI) in the images. In this case, the ROI in each image was the area enclosed by the quadrat, and the area outside of the quadrat was labelled *"out"*, regardless of whether it included macroalgae or not. In the example, from the picture acquired (Figure 5.a), only four polygons corresponding to three different classes were labelled when the expert polygonised the largest relevant macroalgae (Figure 5b). In this case the polygons did not cover all pixels corresponding to each macroalga. A label was then assigned to each pixel (Figure 5c). The contours of the macroalgae were more detailed than those of the respective polygons.

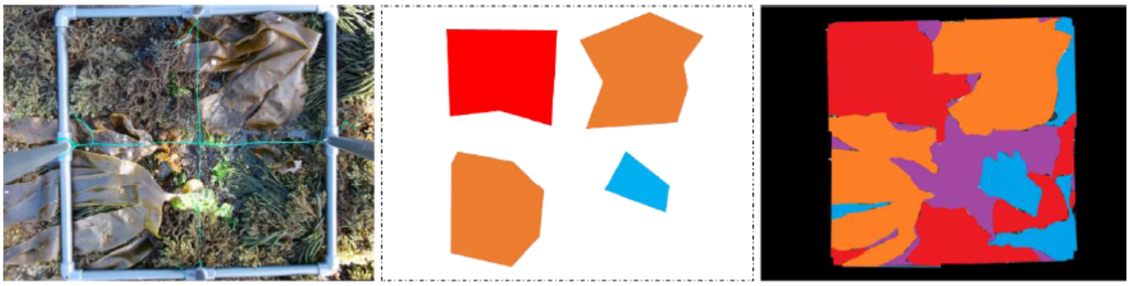

a) b) c)

Figure 5. Types of labelled data: a) geo-referenced and acquired data, b) polygons labelled and selected for training in GIS software, c) raster data for training a semantic segmentation CNN. Classes are represented by different colours.

2.2.2. *Semantic segmentation*

Semantic segmentation and object detection are classification methods that can be applied to image segmentation and labelling (Ruiz-Santaquiteria et al., 2020). Although both methods are based on deep learning, semantic segmentation aims to assign classes to each pixel of the image while the detector frames the detected objects in a bounding box. This bounding box is defined by a fixed number of vertices that frequently cover several pixels that do not correspond to the class detected. Such misclassification is usual in complex scenarios with contiguous classes, as in the case of distribution of macroalgae. Semantic segmentation delineates the classes more precisely, because it is a pixel-based classification, and it was therefore selected as the classification method for this research.

In this paper, we compared the performance of three CNNs in relation to semantic segmentation: MobileNetV2, Resnet18, Xception. These networks each represent different architectures and perform well in segmentation/classification problems. In addition, the training cost of all three CNN is low, both in computational cost and number of labelled samples, as indicated by the number of hidden layers and adjustable parameters. Labelling a large number of samples is a tedious manual task that requires time from biologists familiar with differentiation of macroalgal species. In addition, many laboratories and professionals do not have access to expensive servers to train more complex neural networks, and they are limited to employ personal computers. The characteristics of the different CNNs are summarised below:

- MobilNetv2. This CNN is specially designed for operating on mobile devices, and the ratio between accuracy and cost of training is therefore particularly high. It consists of 53 layers and only 3.5 million adjustable parameters and is based on an inverted residual structure in which the shortcut connections are between the thin bottleneck layers (Sandler et al., 2018).
- ResNet18. This is the shallowest of the Deep Residual Networks. It has 18 layers and 11.7 million adjustable parameters. The most important aspect of this CNN is that, during training, it can skip layers if it considers that feature extraction does not contribute relevant information (He et al., 2016).
- Xception. This is an evolution of Inception architecture. It has 71 layers and 22.9 million adjustable parameters, and is thus the deepest of the networks used in this study. This CNN is based entirely on depth-wise separable convolution layers (Chollet, 2017).

Images for semantic segmentation with CNN must have minimum dimensions according to the feature extractor (224x224x3 pixels for MobilNetv2 and ResNet18, and 299x299x3 pixels for Xception). In the present study, the dimensions of the acquired images were 4288 x 3216 x 3 pixels. Given this high resolution, the images contained a great deal of detail, facilitating manual labelling by experts. Unfortunately, the amount of computer resources that must be allocated for network training increases with the image size. In order to train the networks on a conventional computer, the images were re-sized maintaining the aspect ratio to 1000 x 750 x 3 pixels. This resolution still retained a high level of detail in the images. CNNs were adapted from image classification for semantic segmentation using DeepLabV3 (Chen et al., 2018) in Matlab.

2.2.3. *Data augmentation and distribution*

The data set was also modified by data augmentation. Data augmentation allows the training set to be extended to automatically generate new samples through small modifications of the original set. In this case, data augmentation was applied from reflections on the X and Y axes, 20-pixel translations in both axes and rotations with angles less than 25º.

One aim of the data acquisition process was to obtain a representative number of images of each species. Nevertheless, the percentage occupation of each image was unbalanced (Table 1), which is a typical problem in semantic segmentation. Although almost all classes were of the same order of magnitude, relative to other species, there were very few samples of *S. muticum*. The *"out"* class included a larger number of pixels, as it appeared in all images outside the ROI. The imbalance between classes can be minimized by assigning weights to the pixels according to the quantity in the training set. For the validation and testing sets, balanced sample sets were chosen so that the results were as balanced as possible. In total, 130 images were labelled and distributed as follows: 90 images for training, 10 images for validation and 30 images for testing.

Table 1. Number of pixels per class.

Class	Total number of pixels (10^6)	Training number of pixels (10^6)	Validation number of pixels (10^6)	Testing number of pixels (10^6)
"out"	58.93	41.16	4.47	13.29
B. bifurcata	6.28	4.46	0.47	1.34
C. tamariscifolia	4.96	3.50	0.68	0.77
S. muticum	1.36	0.59	0.30	0.47
S. polyschides	8.33	6.10	0.59	1.63
***Codium* spp**	5.89	3.43	0.46	2.00
"others"	11.76	8.25	0.52	2.99

2.2.4. *Training*

The network was trained on a laptop computer (GPU NVIDIA GTX1050 4GB GDDR5, CPU i7-7700HQ 2.8Ghz and 16GB RAM DDR4). The hyperparameters were chosen experimentally through several tests, maximizing the performance and minimizing the overfitting. The hyperparameters that obtained a better result for training were as follows: optimization method, *sgdm*; learning rate, 0.001; momentum, 0.9; L2 regularization, 0.005; and max epochs, 15. The mini batch size was set at 4 limited by the amount of memory of the graphic card. The time consumed by each training was around 150 min. The programming language used was *Matlab*. All training sessions converged satisfactorily (Figure 6).

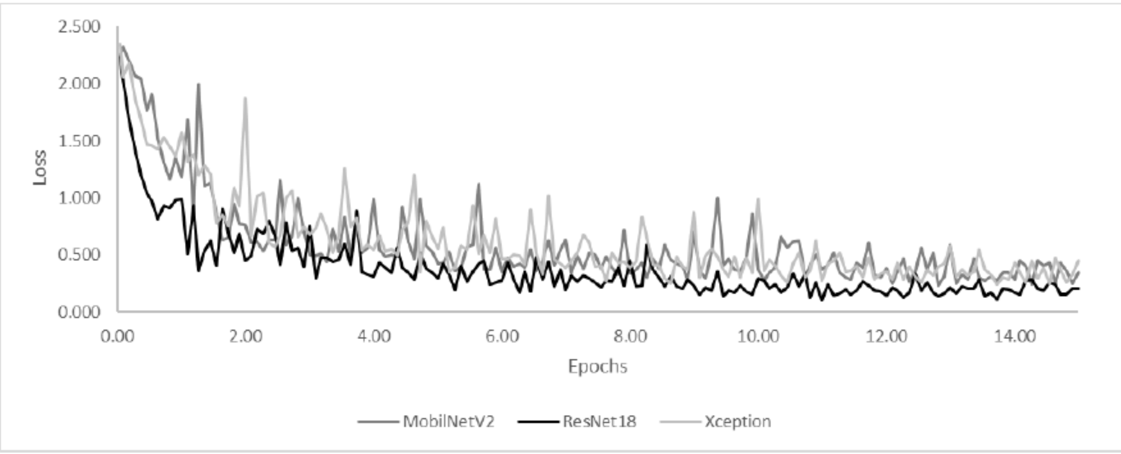

Figure 6. Variation in the loss during the training process

3. Results

Table 2. Overall accuracy obtained on training, validation and test sets.

	Train	**Val**	**Test**
ResNet18	93.7%	90.6%	91.9%
MobileNetV2	91.4%	85.0%	88.4%
Xception	90.9%	84.7%	87.3%

Overall accuracy obtained on training, validation and test sets are shown in Table 2. Overfitting was detected among the training and validation sets, although it was reduced in the testing set. The difference between the validation and test sets is due to the difference in the number of pixels per class. Although the overfitting was reduced with the adjustment of the hyperparameters, it was not completely eliminated. The remaining overfitting was considered acceptable in view of the results, both qualitative and quantitative. The best result was obtained with Resnet18, although the performance was not the same for all classes. The confusion matrices for training the three different CNNs are shown in Tables 3 to 5. The best result was obtained with Resnet18, although the performance was not the same for all classes. ResNet18 produced better segmentation of the *B. bifurcata*, *S. muticum*, *S. polyschides,* and "out" classes. Accurate identification of the "out" class led to good ROI delimitation. MobileNetV2 produced better segmentation of the *Codium* spp and "others" (mainly composed of sand) classes, but produced very similar results to ResNet18. Xception produced by far the best results for the *C. tamariscifolia* class. In the confusion matrices, the success rates were lowest for the *C. tamariscifolia* and *S. muticum* classes, which yielded more confusion than the other classes. Specifically, *C. tamariscifolia* was confused with the "others" classes by 0.296, and *S. muticum* was confused with the "others" by 0.197, and with *C. tamariscifolia* by 0.141. The colours of these classes were similar; in addition, very few samples of the *S. muticum* class were available for training. Good success rates were obtained for the remaining classes, and the confusion between them was minimal.

The most notable results for semantic segmentation with ResNet18 were the areas classified as macroalgae outside the ROI (Figure 7). However, these areas corresponded to macroalgae that were well classified and with continuous macroalgae within the ROI. In addition, although the centres of the macroalgae were well defined, the borders were quite irregular and not well defined. The borders did not fit properly, mainly in dark areas, overlapping areas between macroalgae or when a small macroalga was surrounded by another macroalga.

Resnet18 produced the best segmentation of macroalgae. It was foreseeable that MobileNetv2 would not perform particularly well, given the fewer configurable parameters. However, Xception did not produce better results, despite being a much deeper CNN with the capacity to extract more complex features. The Xception network only outperformed the other CNNs in the accuracy of segmenting the *C. tamariscifolia* class (one of the classes for which ResNet18 produced the least accurate results), but at the cost of increasing confusion about the *S. muticum* class, for which relatively poor results were obtained.

Very high success rates were obtained for the segmentation of most classes (including three different macroalgal species). ResNet18 learned the texture and colour patterns of different species, regardless of factors that led to changes, such as the time out of water between acquisitions. Although the *B. bifurcata* and *Codium spp* classes were of similar texture, they were easily distinguished by their colour. The *S. polyschides* class did not coincide in colour or texture with any of the other classes. Low success rates (of around 60%), were only obtained for the *C. tamariscifolia* and *S. muticum* classes, possibly due to the similar colour and texture of these species.

Table 3. Confusion matrix for ResNet18.

ref\pred	**"out"**	***B. bifurcata***	***C. tamariscifolia***	***S. muticum***	***S. polyschides***	***Codium* spp**	**"others"**
"out"	**0.962**	0.004	0.001	0.001	0.012	0.010	0.009
B. bifurcata	0.003	**0.921**	0.002	0.009	0.001	0.007	0.058

C. tamariscifolia	0.004	0.020	**0.590**	0.042	0.017	0.032	0.296
S. muticum	0.015	0.008	0.197	**0.618**	0.018	0.004	0.141
S. polyschides	0.008	0.003	0.004	0.000	**0.939**	0.019	0.026
***Codium* spp**	0.003	0.010	0.012	0.002	0.026	**0.912**	0.034
"others"	0.008	0.025	0.032	0.004	0.025	0.052	**0.854**

Table 4. Confusion matrix for MobileNetV2.

ref\pred	**"out"**	***B. bifurcata***	***C. tamariscifolia***	***S. muticum***	***S. polyschides***	***Codium* spp**	**"others"**
"out"	**0.902**	0.008	0.005	0.004	0.023	0.027	0.032
B. bifurcata	0.007	**0.907**	0.006	0.007	0.002	0.014	0.058
C. tamariscifolia	0.003	0.016	**0.606**	0.039	0.009	0.013	0.314
S. muticum	0.031	0.006	0.121	**0.601**	0.005	0.008	0.229
S. polyschides	0.016	0.003	0.007	0.000	**0.899**	0.027	0.048
***Codium* spp**	0.007	0.007	0.009	0.003	0.020	**0.926**	0.028
"others"	0.012	0.016	0.034	0.004	0.018	0.044	**0.871**

Table 5. Confusion matrix for Xception.

ref\pred	**out**	***B. bifurcata***	***C. tamariscifolia***	***S. muticum***	***S. polyschides***	***Codium* spp**	**"others"**
"out"	**0.908**	0.012	0.008	0.001	0.019	0.021	0.031
B. bifurcata	0.004	**0.884**	0.020	0.000	0.001	0.014	0.077
C. tamariscifolia	0.006	0.019	**0.725**	0.003	0.009	0.031	0.206
S. muticum	0.017	0.014	0.500	**0.266**	0.003	0.010	0.190
S. polyschides	0.016	0.011	0.008	0.000	**0.878**	0.026	0.060
***Codium* spp**	0.009	0.010	0.027	0.001	0.019	**0.899**	0.036
"others"	0.011	0.023	0.076	0.002	0.017	0.042	**0.829**

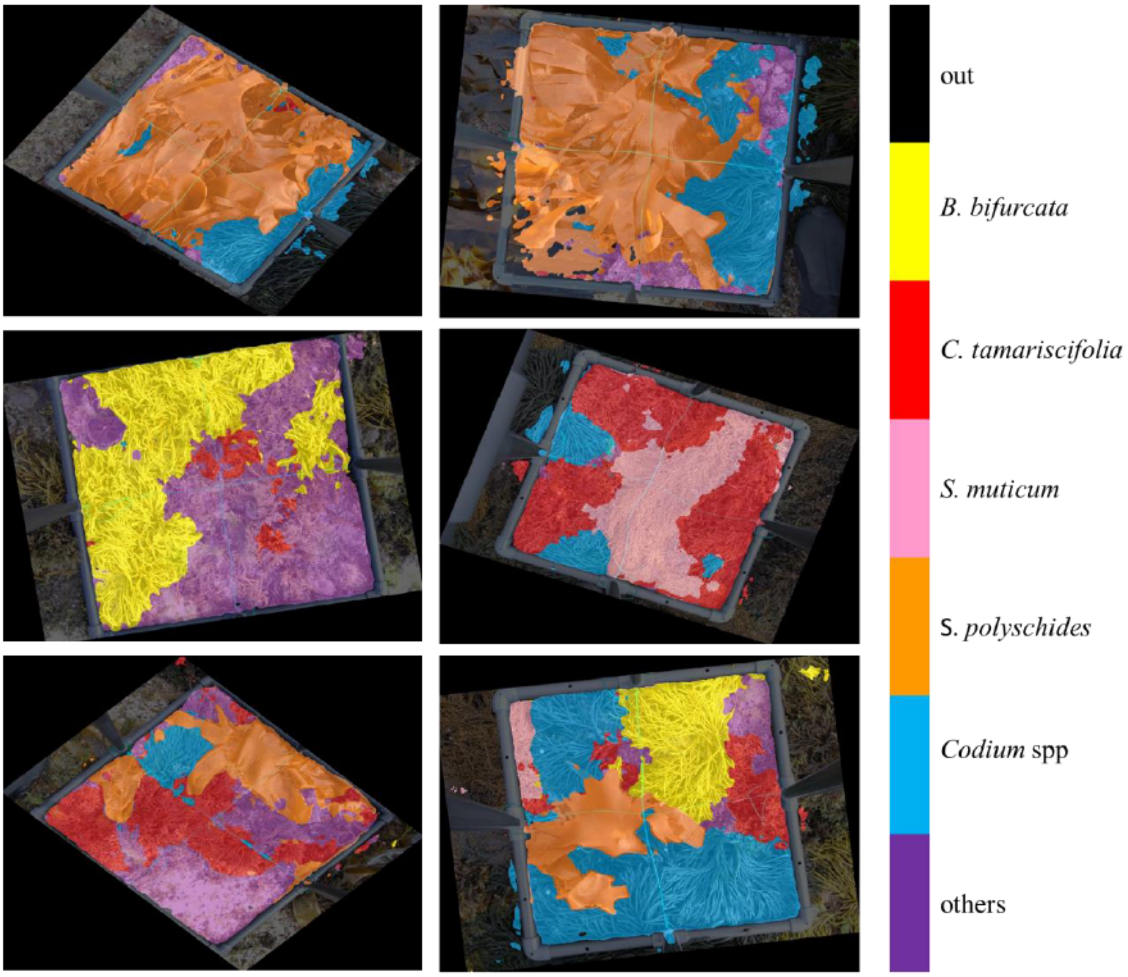

Figure 7. Results of semantic segmentation with ResNet18. The acquired image was superimposed on colours representing each class.

4. Discussion

In this paper, we report a CNN-based segmentation procedure for macroalgae, which yielded a success rate > 90% for all three CNNs tested. One of the key reasons for the high success rate in classifying the species was the use of high-resolution ground images collected in the field. The images were reduced in order to save time and computational resources, to a final resolution of 1000 x 750 pixels, which was high relative to the examples reported in the literature. By contrast, underwater images used to segment seagrass coverage were reduced to 512 x 256 pixels in previous studies (Weidmann et al., 2019). The study findings show that the proposed resolution satisfactory differentiated the five species and the interior/exterior zones of each quadrat. At the same time, a laptop workstation was adequate for training the CNNs at this resolution, and computational resources from external servers were not required.

Although the accuracy rate was similar to that obtained in other studies with satellite, aerial and submarine sources, the present study aimed to differentiate five different macroalgae and it is, therefore, not generally comparable to other studies concerning the detection of single species. The accuracy achieved in number of CNN-based studies is very variable: 99.4% (Zhou et al., 2019), 97.0% (Wang et al., 2019), 95.8% (Rahnemoonfar and Dobbs, 2019), 95.0% (Martin-Abadal et al., 2018) and 90.1% (Arellano-Verdejo et al., 2018). These studies usually based on satellite and airborne data have only focused on detecting the predominant macroalgal species given the low resolution relative to ground data. Their technical complexity is considerably lesser than the presented in this work. They segmented of one macroalgae class from the bottom, often sand or water, without differentiation between macroalgal species. Differentiating between different macroalgal species is feasible when broad taxonomic groups are considered, e.g. green, red and brown algae (Andrefouet et al., 2004; Kotta et al., 2018). The findings of the present study showed that colour attributes were not sufficient for correct classification, as *C. tamariscifolia* and *S. muticum* are very similar in colour and only differ in texture. Depending on the classification scale, the texture feature is not extractable from satellite and aerial images due to the lower resolution of these. In addition, the same species can display notable differences in colour depending on the morphology, thickness of thalli and cellular architecture, which determine pigment densities, absorption, and thus reflectance spectra (Vogelmann and Björn, 1986). Environmental conditions, such as the emersion time and intensity of solar radiation, also contribute to differences in pigmentation within and between macroalgal species (Dieter et al., 2003). The resolution of images obtained by underwater drones is higher than that of airborne data, and the colour is modified relative to images taken outside the water; however, the modification affects all species equally (O'Byrne et al., 2018). Macroalgal species should be able to be differentiated by these characteristics (resolution and colour), and therefore texture, in underwater images. Nevertheless, most studies based on underwater images and also studies based on satellite and aerial images have only focused on detecting single macroalgal species (Gonzalez-Cid et al., 2017; Moniruzzaman et al., 2019).

The features extracted from one species were easier to obtain and learn with a classifier based on artificial intelligence, as the macroalgal classes shared more features with each other than with non-macroalgal classes such as rock, sand and seawater. However, when the macroalgal class no longer corresponded to one species (as in this study) and was divided into five classes, the difficulty for the algorithm increased in relation to both finding and in extracting distinctive features. More advanced techniques than simple Support Vector Machines or Artificial Neural Networks were thus required. Classic image processing techniques such as LBP lack the ability to learn complex features and thus produce poorer results than those obtained with CNNs. The accuracy of segmentation of single seagrass species only reaches 85.0% with LBP techniques, but increases to 93.4% with CNN (Wang et al., 2018; Reus et al., 2018).

The CNNs under study proved very useful for segmentation of the five macroalgae considered. Although, in theory, a large number of labelled images was required, in practice the number of pixels was more important for semantic segmentation. Given the high resolution of the images used, the number of pixels was sufficient to train a CNN with only 100 images, which can be obtained quickly. From these 100 labelled images, and after training, infinite images can be labelled without further human intervention. However, the labelling process for training must be conducted carefully, as CNNs can learn labelling errors. Confusion at the borders of macroalgae (Figure 7) was due to labelling errors of the images (Vogelmann and Björn, 1986). For human observers, the centre of the algae is easy to segment and label manually, as with CNN segmentation. However, the borders of many algae overlap and it is not easy to define outlines to separate them. Because of these errors in the labelled images, the errors were also learnt by the CNN and replicated in the segmentation. These types of errors tend to be minimized when the data are tagged by different people.

The acquisition time is slower with ground imaging than in satellite and drone-based methods, because the quadrat has constantly to be moved to a new location for each new image. In addition, the area covered by each image was only 0.25 m^2. Nevertheless, ground images are required in order to provide reference data to train models and map data obtained with other automated instruments. This study focused on the exclusive use of RGB photographic images to minimize pre-processing time by fusing information and acquisition efforts. Because of the high success rates obtained, other types of data, such as spectroradiometer data (Hu, 2009), multispectral-hyperspectral images (Fauzan et al., 2017; Li et al., 2012; Taddia et al., 2019; Zacharias et al., 1992) and environmental data (De Oliveira et al., 2006), were not included.

5. Conclusion and future work

This study involved a CNN-based semantic segmentation of high-resolution ground images of five different macroalgae inhabiting rocky shores. The study findings demonstrate that vector-labelled samples can be adapted for use with CNNs. Of the three different CNNs compared, ResNet18 produced the best results, i.e. 91.9% accuracy. Most of the samples were correctly labelled, although there was a tendency for some macroalgae outside the ROI to be labelled, and the borders between macroalgal species were diffuse. Although theoretically considered an error, in practice segmentation of macroalgae outside the ROI is not problematical, as long as the classification is correct, as in this case. Definition of borders is also a problem experienced by human observers. The proposed method is therefore considered a suitable alternative for the automation of sample labelling.

The study findings demonstrated that automation of the labelling process is possible with only 100 high-resolution images obtained in the field, without the need for other types of data. A further step will be to apply the method to data obtained from UAVs. Nevertheless, further research is required to determine the minimum resolution needed to guarantee correct results and for transfer to learning between UAV and ground images, which differ in resolution and, therefore, in texture and colour. The use of UAVs, together with the findings presented here, will facilitate the rapid acquisition and mapping of macroalgal cover on intertidal rocky shores, with a high degree of automation. Use of these methods could greatly improve the management of coastal areas.

Acknowledgements

This work was supported by the Fundación Biodiversidad, the Ministerio para la Transición Ecológica y el Reto Demográfico through the Pleamar program, co-funded by the European Maritime and Fisheries Fund (EMFF), call 2018. It was also partly funded through grants awarded by the Xunta de Galicia for human resources and competitive reference groups (ED481B-2019-061 and ED431C 2016-038) and by the Ministerio de Ciencia, Innovación y Universidades -Gobierno de España (RTI2018-095893-B-C21). This document only reflects the views of the authors, and the statements made herein are solely the responsibility of the authors.

References and Notes

Adeniyi, O.M., Azimov, U., Burluka, A., 2018. Algae biofuel: Current status and future applications. Renewable and Sustainable Energy Reviews 90, 316–335. https://doi.org/https://doi.org/10.1016/j.rser.2018.03.067

Andrefouet, S., Payri, C., Hochberg, E., Hu, C., Atkinson, M., Muller-Karger, F., 2004. Use of In Situ and Airborne Reflectance for Scaling-Up Spectral Discrimination of Coral Reef Macroalgae from Species to Communities. Marine Ecology-progress Series - MAR ECOL-PROGR SER 283, 161–177. https://doi.org/10.3354/meps283161

Arellano-Verdejo, J., Lazcano, H., Cabanillas-Terán, N., 2018. ERISNet: Deep learning network for Sargassum detection along the coastline of the Mexican Caribbean. https://doi.org/10.7287/peerj.preprints.27445

Bañolas, G., Fernández, S., Espino, F., Haroun, R., Tuya, F., 2020. Evaluation of carbon sinks by the seagrass Cymodocea nodosa at an oceanic island: Spatial variation and economic valuation. Ocean & Coastal Management 187, 105112. https://doi.org/https://doi.org/10.1016/j.ocecoaman.2020.105112

Beaumont, N., Austen, M., Mangi, S., Townsend, M., 2008. Economic valuation for the conservation of marine biodiversity. Marine pollution bulletin 56, 386–396. https://doi.org/10.1016/j.marpolbul.2007.11.013

Brodie, J., Ash, L., Tittley, I., Yesson, C., 2018. A comparison of multispectral aerial and satellite imagery for mapping intertidal seaweed communities. Aquatic Conservation: Marine and Freshwater Ecosystems 28. https://doi.org/10.1002/aqc.2905

Casal, G., Kutser, T., Gómez, J., Sánchez-Carnero, N., Freire, J., 2013. Assessment of the hyperspectral sensor CASI-2 for macroalgal discrimination on the Ría de Vigo coast (NW Spain) using field spectroscopy and modelled spectral libraries. Continental Shelf Research 55, 129–140. https://doi.org/10.1016/j.csr.2013.01.010

Chen, L.-C., Zhu, Y., Papandreou, G., Schroff, F., Adam, H., 2018. Encoder-decoder with atrous separable convolution for semantic image segmentation, in: Proceedings of the European Conference on Computer Vision (ECCV). pp. 801–818.

Chollet, F., 2017. Xception: Deep Learning with Depthwise Separable Convolutions, in: 2017 IEEE Conference on Computer Vision and Pattern Recognition (CVPR). pp. 1800–1807. https://doi.org/10.1109/CVPR.2017.195

De Oliveira Eric Populus Jacques, G.B., 2006. Predictive modelling of coastal habitats using remote sensing data and fuzzy logic: A case for seaweed in Brittany (France). EARSeL eProceedings.

Debiagi, P., Trinchera, M., Frassoldati, A., Ranzi, E., Faravelli, T., 2017. Third Generation Biomass. Classification and Characterization of Algae Fuels.

Dieter, H., Wiencke, C., Bischof, K., 2004. Photosynthesis in Marine Macroalgae. pp. 413–435. https://doi.org/10.1007/978-94-007-1038-2_18

Duarte, L., Viejo, R.M., Martínez, B., deCastro, M., Gómez-Gesteira, M., Gallardo, T., 2013. Recent and historical range shifts of two canopy-forming seaweeds in North Spain and the link with trends in sea surface temperature. Acta Oecologica 51, 1–10. https://doi.org/https://doi.org/10.1016/j.actao.2013.05.002

Duffy, J.P., Pratt, L., Anderson, K., Land, P.E., Shutler, J.D., 2018. Spatial assessment of intertidal seagrass meadows using optical imaging systems and a lightweight drone. Estuarine, Coastal and Shelf Science 200, 169–180. https://doi.org/https://doi.org/10.1016/j.ecss.2017.11.001

Fauzan, M.A., Kumara, I.S.W., Yogyantoro, R., Suwardana, S., Fadhilah, N., Nurmalasari, I., Apriyani, S., Wicaksono, P., 2017. Assessing the Capability of Sentinel-2A Data for Mapping Seagrass Percent Cover in Jerowaru, East Lombok. The Indonesian Journal of Geography 49, 195–203.

Floor, J.R., van Koppen, C.S.A. (Kris), van Tatenhove, J.P.M., 2018. Science, uncertainty and changing storylines in nature restoration: The case of seagrass restoration in the Dutch Wadden Sea. Ocean & Coastal Management 157, 227–236. https://doi.org/https://doi.org/10.1016/j.ocecoaman.2018.02.016

Gonzalez-Cid, Y., Burguera, A., Bonin-Font, F., Matamoros, A., 2017. Machine learning and deep learning strategies to identify Posidonia meadows in underwater images, in: OCEANS 2017 - Aberdeen. pp. 1–5. https://doi.org/10.1109/OCEANSE.2017.8084991

Griffiths, L.L., Connolly, R.M., Brown, C.J., 2020. Critical gaps in seagrass protection reveal the need to address multiple pressures and cumulative impacts. Ocean & Coastal Management 183, 104946. https://doi.org/https://doi.org/10.1016/j.ocecoaman.2019.104946

Hawkins, S., Sugden, H., Mieszkowska, N., Moore, P., Poloczanska, E., Leaper, R., Herbert, R., Genner, M., Moschella, P.S., Thompson, R.C., Jenkins, S.R., Southward, A.J., Burrows, M., 2009. Consequences of climate-driven biodiversity changes for ecosystem functioning of North European rocky shores. Marine Ecology Progress Series 396.

He, K., Zhang, X., Ren, S., Sun, J., 2016. Deep residual learning for image recognition, in: Proceedings of the IEEE Conference on Computer Vision and Pattern Recognition. pp. 770–778.

Helmuth, B., Mieszkowska, N., Moore, P., Hawkins, S.J., 2006. Living on the Edge of Two Changing Worlds: Forecasting the Responses of Rocky Intertidal Ecosystems to Climate Change. Annual Review of Ecology, Evolution, and Systematics 37, 373–404. https://doi.org/10.1146/annurev.ecolsys.37.091305.110149

Hu, C., 2009. A novel ocean color index to detect floating algae in the global oceans. Remote Sensing of Environment 113, 2118–2129. https://doi.org/https://doi.org/10.1016/j.rse.2009.05.012

Jenkins, S.R., Moore, P., Burrows, M.T., Garbary, D.J., Hawkins, S.J., Ingólfsson, A., Sebens, K.P., Snelgrove, P.V.R., Wethey, D.S., Woodin, S.A., 2008. Comparative ecology of North Atlantic shores: Do differences in players matter for process? Ecology 89, S3–S23. https://doi.org/10.1890/07-1155.1

Kellaris, A., Gil, A., Faria, J., Amaral, R., Moreu-Badia, I., Neto, A., Yesson, C., 2019. Using low-cost drones to monitor heterogeneous submerged seaweed habitats: A case study in the Azores. Aquatic Conservation: Marine and Freshwater Ecosystems 29, 1909–1922. https://doi.org/10.1002/aqc.3189

Kotta, J., Valdivia, N., Kutser, T., Toming, K., Rätsep, M., Orav-Kotta, H., 2018. Predicting the cover and richness of intertidal macroalgae in remote areas: a case study in the Antarctic Peninsula. Ecology and Evolution 8, 9086–9094. https://doi.org/10.1002/ece3.4463

Lamela-Silvarrey, C., Fernández, C., Anadón, R., Arrontes, J., 2012. Fucoid assemblages on the north coast of Spain: past and present (1977–2007). Botanica Marina. https://doi.org/10.1515/bot-2011-0081

Li, R., Liu, J.-K., Sukcharoenpong, A., Yuan, J., Zhu, H., Zhang, S., 2012. A Systematic Approach toward Detection of Seagrass Patches from Hyperspectral Imagery. Marine Geodesy 35, 271–286. https://doi.org/10.1080/01490419.2012.699019

Lima, F.P., Ribeiro, P.A., Queiroz, N., Hawkings, S.J., Santos, A.M., 2007. Do distributional shifts of northern and southern species of algae match the warming pattern? Global Change Biology 13, 2592–2604. https://doi.org/10.1111/j.1365-2486.2007.01451.x

Macreadie, P.I., Jarvis, J., Trevathan-Tackett, S.M., Bellgrove, A., 2017. Seagrasses and Macroalgae: Importance, Vulnerability and Impacts. Climate Change Impacts on Fisheries and Aquaculture, Wiley Online Books. https://doi.org/doi:10.1002/9781119154051.ch22

Martin-Abadal, M., Guerrero-Font, E., Bonin-Font, F., Gonzalez-Cid, Y., 2018. Deep Semantic Segmentation in an AUV for Online Posidonia Oceanica Meadows Identification. IEEE Access 6, 60956–60967. https://doi.org/10.1109/ACCESS.2018.2875412

Matias, M.G., Arenas, F., Rubal, M., Pinto, I.S., 2015. Macroalgal Composition Determines the Structure of Benthic Assemblages Colonizing Fragmented Habitats. PloS one 10, e0142289–e0142289. https://doi.org/10.1371/journal.pone.0142289

Moniruzzaman, M., Islam, S.M.S., Lavery, P., Bennamoun, M., 2019. Faster R-CNN Based Deep Learning for Seagrass Detection from Underwater Digital Images, in: 2019 Digital Image Computing: Techniques and Applications (DICTA). pp. 1–7. https://doi.org/10.1109/DICTA47822.2019.8946048

O'Byrne, M., Pakrashi, V., Schoefs, F., Ghosh, B., 2018. Semantic Segmentation of Underwater Imagery Using Deep Networks Trained on Synthetic Imagery. Journal of Marine Science and Engineering . https://doi.org/10.3390/jmse6030093

Park, J.B.K., Craggs, R.J., Shilton, A.N., 2011. Wastewater treatment high rate algal ponds for biofuel production. Bioresource Technology 102, 35–42. https://doi.org/https://doi.org/10.1016/j.biortech.2010.06.158

Pittman, J.K., Dean, A.P., Osundeko, O., 2011. The potential of sustainable algal biofuel production using wastewater resources. Bioresource Technology 102, 17–25. https://doi.org/https://doi.org/10.1016/j.biortech.2010.06.035

Purvaja, R., Robin, R.S., Ganguly, D., Hariharan, G., Singh, G., Raghuraman, R., Ramesh, R., 2018. Seagrass meadows as proxy for assessment of ecosystem health. Ocean & Coastal Management 159, 34–45. https://doi.org/https://doi.org/10.1016/j.ocecoaman.2017.11.026

Quiros, T.E.A.L., Beck, M.W., Araw, A., Croll, D.A., Tershy, B., 2018. Small-scale seagrass fisheries can reduce social vulnerability: a comparative case study. Ocean & Coastal Management 157, 56–67. https://doi.org/https://doi.org/10.1016/j.ocecoaman.2018.02.003

Rahnemoonfar, M., Dobbs, D., 2019. SEMANTIC SEGMENTATION OF UNDERWATER SONAR IMAGERY WITH DEEP LEARNING. https://doi.org/10.13140/RG.2.2.32343.52644

Rebours, C., Marinho-Soriano, E., Zertuche-González, J.A., Hayashi, L., Vásquez, J.A., Kradolfer, P., Soriano, G., Ugarte, R., Abreu, M.H., Bay-Larsen, I., others, 2014. Seaweeds: an opportunity for wealth and sustainable livelihood for coastal communities. Journal of applied phycology 26, 1939–1951.

Reus, G., Moller, T., Jager, J., Schultz, S., Kruschel, C., Hasenauer, J., Wolff, V., Fricke-Neuderth, K., 2018. Looking for Seagrass: Deep Learning for Visual Coverage Estimation. https://doi.org/10.1109/OCEANSKOBE.2018.8559302

Ruiz-Santaquiteria, J., Bueno, G., Deniz, O., Vallez, N., Cristobal, G., 2020. Semantic versus instance segmentation in microscopic algae detection. Engineering Applications of Artificial Intelligence 87, 103271. https://doi.org/https://doi.org/10.1016/j.engappai.2019.103271

Sagawa, T., Mikami, A., Aoki, M., Komatsu, T., 2012. Mapping seaweed forests with IKONOS image based on bottom surface reflectance, Proceedings of SPIE - The International Society for Optical Engineering. https://doi.org/10.1117/12.975678

Sandler, M., Howard, A., Zhu, M., Zhmoginov, A., Chen, L., 2018. MobileNetV2: Inverted Residuals and Linear Bottlenecks, in: 2018 IEEE/CVF Conference on Computer Vision and Pattern Recognition. pp. 4510–4520. https://doi.org/10.1109/CVPR.2018.00474

Schroeder, S.B., Dupont, C., Boyer, L., Juanes, F., Costa, M., 2019. Passive remote sensing technology for mapping bull kelp (Nereocystis luetkeana): A review of techniques and regional case study. Global Ecology and Conservation 19, e00683. https://doi.org/https://doi.org/10.1016/j.gecco.2019.e00683

Siddiqui, D.M., Zaidi, Z.A., Abdullah, M., 2019. Performance Evaluation of Newly Proposed Seaweed Enhancing Index (SEI). Remote Sensing . https://doi.org/10.3390/rs11121434

Smale, D.A., Burrows, M.T., Moore, P., O'Connor, N., Hawkins, S.J., 2013. Threats and knowledge gaps for ecosystem services provided by kelp forests: a northeast Atlantic perspective. Ecology and Evolution 3, 4016–4038. https://doi.org/10.1002/ece3.774

Taddia, Y., Russo, P., Lovo, S., Pellegrinelli, A., 2019. Multispectral UAV monitoring of submerged seaweed in shallow water. Applied Geomatics. https://doi.org/10.1007/s12518-019-00270-x

Tamondong, A., Cruz, C., Guihawan, J., Garcia, M., Quides, R.R., Cruz, J., Blanco, A., 2018. Remote sensing-based estimation of seagrass percent cover and LAI for above ground carbon sequestration mapping. https://doi.org/10.1117/12.2324695

Topouzelis, K., Spondylidis, S.C., Papakonstantinou, A., Soulakellis, N., 2016. The use of Sentinel-2 imagery for seagrass mapping: Kalloni Gulf (Lesvos Island, Greece) case study, in: Proc.SPIE.

Ventura, D., Bonifazi, A., Gravina, F.M., Belluscio, A., Ardizzone, G., 2018. Mapping and Classification of Ecologically Sensitive Marine Habitats Using Unmanned Aerial Vehicle (UAV) Imagery and Object-Based Image Analysis (OBIA). Remote Sensing . https://doi.org/10.3390/rs10091331

Vogelmann, T.C., Björn, L.O., 1986. Plants as light traps. Physiologia Plantarum 68, 704–708. https://doi.org/10.1111/j.1399-3054.1986.tb03421.x

Wang, M., Fei, X., Zhang, Y., Chen, Z., Wang, X., Tsou, Y.J., Liu, D., Lu, X., 2018. Assessing Texture Features to Classify Coastal Wetland Vegetation from High Spatial Resolution Imagery Using Completed Local Binary Patterns (CLBP). Remote Sensing . https://doi.org/10.3390/rs10050778

Wang, S., Liu, L., Qu, L., Yu, C., Sun, Y., Gao, F., Dong, J., 2019. Accurate Ulva prolifera regions extraction of UAV images with superpixel and CNNs for ocean environment monitoring. Neurocomputing 348, 158–168. https://doi.org/https://doi.org/10.1016/j.neucom.2018.06.088

Weidmann, F., Jäger, J., Reus, G., Schultz, S.T., Kruschel, C., Wolff, V., Fricke-Neuderth, K., 2019. A Closer Look at Seagrass Meadows: Semantic Segmentation for Visual Coverage Estimation, in: OCEANS 2019 - Marseille. pp. 1–6. https://doi.org/10.1109/OCEANSE.2019.8867064

Wilson, K.L., Skinner, M.A., Lotze, H.K., 2019. Eelgrass (Zostera marina) and benthic habitat mapping in Atlantic Canada using high-resolution SPOT 6/7 satellite imagery. Estuarine, Coastal and Shelf Science 226, 106292. https://doi.org/https://doi.org/10.1016/j.ecss.2019.106292

Xing, Q., An, D., Zheng, X., Wei, Z., Wang, X., Li, L., Tian, L., Chen, J., 2019. Monitoring seaweed aquaculture in the Yellow Sea with multiple sensors for managing the disaster of macroalgal blooms. Remote Sensing of Environment 231, 111279. https://doi.org/https://doi.org/10.1016/j.rse.2019.111279

Zacharias, M., Niemann, O., Borstad, G., 1992. An Assessment and Classification of a Multispectral Bandset for the Remote Sensing of Intertidal Seaweeds. Canadian Journal of Remote Sensing 18, 263–274. https://doi.org/10.1080/07038992.1992.10855331

Zhou, Y., Wang, J., Li, B., Meng, Q., Rocco, E., Saiani, A., 2019. Underwater scene segmentation by deep neural network.